

The vacuum UV photoabsorption spectroscopy of the geminal ethylene difluoride (1,1-C₂H₂F₂). The vibrational structure and its analysis

R. Locht^a, H.W. Jochims^b, B. Leyh^a

^a *Molecular Dynamics Laboratory, Department of Chemistry, Building B6c, University of Liège, Sart-Tilman, B-4000 Liège 1, Belgium*

^b *Institut für Physikalische und Theoretische Chemie, Freie Universität Berlin, Takustraße 3, D-14195 Berlin, Germany*

ABSTRACT

The vacuum UV photoabsorption spectrum of 1,1-C₂H₂F₂ has been examined in detail between 6 eV and 25 eV photon energy by using synchrotron radiation. The broad band observed at 7.52 eV includes the $\pi \rightarrow \pi^*$ and the $2b_1 \rightarrow 3s$ Rydberg transitions. An analysis is proposed and applied to the fine structure belonging to these transitions. For the $\pi(2b_1) \rightarrow \pi^*$ transition, one long vibrational progression is observed with $\omega_2 = 1475 \pm 80 \text{ cm}^{-1}$ combined with one quantum of vibration of $\omega_4 = 976 \pm 24 \text{ cm}^{-1}$ and its adiabatic excitation energy is determined at 6.742 eV. The $2b_1 \rightarrow 3s$ Rydberg transition is characterized by a single progression with $\omega_2 = 1532 \pm 80 \text{ cm}^{-1}$ starting at 6.957 eV. These vibrations are ascribed to the C=C and C-F stretching motions respectively. The abundant structure observed between 8.2 eV and 11.2 eV has been analyzed in terms of vibronic transitions to ns ($\delta = 0.98$) and two different np ($\delta = 0.50$ and 0.31) and nd ($\delta = 0.13$ and 0.044) Rydberg series all converging to the 1,1-C₂H₂F₂⁺(\tilde{X}^2B_1) ionic ground state. An analysis of the associated vibrational structure of the individual Rydberg states has been attempted providing average values of the wavenumbers $\omega_2 = 1549 \pm 16 \text{ cm}^{-1}$, $\omega_4 = 839 \pm 40 \text{ cm}^{-1}$ and $\omega_5 = 589 \pm 16 \text{ cm}^{-1}$. Eight other Rydberg states were also analyzed. The vacuum UV spectrum of 1,1-C₂H₂F₂ has been recorded for the first time above 11.2 eV and up to 25 eV. Several broad and strong bands are tentatively assigned to transitions to Rydberg states which are members of Rydberg series converging to excited ionic states of 1,1-C₂H₂F₂. For several of these Rydberg states vibrational structures are observed and assignments are proposed.

Keywords : Vacuum UV photoabsorption spectroscopy ; Synchrotron radiation ; 1,1-C₂H₂F₂ ; Valence transitions ; Rydberg transitions ; Vibrational structure

1. Introduction

The energetic and structural characterization of the neutral as well as the ionic ground and excited states of ethylene and its halogenated derivatives are of considerable interest for understanding the photochemistry of this extremely important class of compounds involved in many fields of pure and applied chemistry. Furthermore, another and more fundamental motivation of such a work is the systematic investigation of the influence of the position and nature of the substituent on the ionization and dissociation dynamics of the molecular ions. The systematic study of ethylene and of several of its halogen substituted derivatives has been initiated or is in progress using vacuum UV photoabsorption and photoelectron spectroscopies [1-3].

The vacuum UV photoabsorption spectroscopic data reported on 1,1-C₂H₂F₂ are very scarce in the literature. To the best of our knowledge, the earliest vacuum UV photoabsorption work on the 1,1-C₂H₂F₂ molecule has been reported by Bélanger and Sandorfy [4] together with five other fluorine substituted ethylenes. This study was restricted to the 50,000-87,100 cm^{-1} (6.2-10.8 eV) spectral region. A classification of the transitions and a vibrational analysis has been proposed.

Dauber and Brith [5] investigated the electronic spectrum of halogen derivatives of ethylene in the vacuum UV region of 150-250 nm (8.26-4.96 eV) in the gas, solid phase and Kr matrix. The existence of $\pi \rightarrow \pi^*$, $\pi \rightarrow \sigma^*$ and Rydberg transitions were discussed. However, these authors put the emphasis of their discussion on the chlorine derivatives.

Reinke et al. [6] measured the low resolution photoabsorption spectrum and the dissociative photoionization of 1,1-C₂H₂F₂ in the vacuum UV range of 10-21 eV using synchrotron radiation. The authors

made a comparison between photoabsorption and the ionization efficiencies of the molecular ion and of the fragment ions, and the photoelectron spectrum is highlighted, too.

The latest detailed photoabsorption work devoted to this molecule has been reported by Limao-Vieira et al. [7]. These authors measured the vacuum UV photoabsorption spectrum of difluorochloromethane (CHClF_2) and of geminal difluoroethylene ($1,1\text{-C}_2\text{H}_2\text{F}_2$) in the same photon energy range (10.8-6.2 eV, 115-200 nm) using synchrotron radiation. Absolute cross-sections were measured. The observed features were classified and assigned to valence \rightarrow valence ($\pi \rightarrow \pi^*$) and to valence \rightarrow Rydberg (ns -, np - and nd -) transitions. A vibrational analysis and assignments of these transitions were presented.

The valence-shell electron energy spectroscopy (VSEES) technique is closely related to vacuum UV photoabsorption spectroscopy. The only work using this technique has been reported by Coggiola et al. [8]. The electron energy spectra of seven fluoroethylene derivatives were reported in the 4.5-16.0 eV electron energy range. At low energy singlet-singlet ($N \rightarrow V$) as well as singlet-triplet ($N \rightarrow T$) transitions have been observed.

Recently, ab initio quantum mechanical calculations have been carried out on $1,1\text{-C}_2\text{H}_2\text{F}_2$ to investigate the neutral excited-state energy surfaces. Excitation energies were calculated at the SACCI (symmetry-adapted cluster configuration interaction) level [9] and compared with the experiment. Several low-lying triplet excited states were also studied. CASSCF (complete active space self-consistent field) calculations corrected with second order perturbation theory (CASPT2) have been used to characterize the valence and 3s and 3p Rydberg states [10]. Furthermore, the existence of several conical intersections has been demonstrated for different geometries.

The ionization and dissociative photoionization dynamics of $1,1\text{-C}_2\text{H}_2\text{F}_2$ have already been investigated in this laboratory by photoelectron spectroscopies (PES) [3], threshold photoelectron-photoion coincidence spectroscopy (TPEPICO) [11] and photoionization mass spectrometric ion translational energy analysis by the maximum entropy method (MEM) [12].

To complete the work on this molecular system, the aim of this paper is to report the vacuum UV photoabsorption spectrum of $1,1\text{-C}_2\text{H}_2\text{F}_2$ (i) for the first time in the 10.5-25 eV photon energy range at medium resolution and (ii) in the 6.0-11.2 eV spectral region at higher resolution. The vibrational structure observed in both regions will be analyzed in detail.

2. Experimental

2.1. Experimental setup

The experimental setup used in this work has already been described in detail elsewhere [13]. Only the most salient features will be reported here.

Synchrotron radiation available from the BESSY I facility (Berlin, Germany) was dispersed with a modified vacuum UV normal incidence 225 McPherson monochromator with a focal length of 1.5 m, instead of 1 m in the commercial version (1m-NIM-2 beam line). A laminar Zeiss grating is used for the efficient reduction of the 2nd spectral order. It is gold coated with 1200 lines mm^{-1} and its transmission breaks down above 26 eV (210,000 cm^{-1} or 48 nm). The width of the entrance and exit slits of 100 μm ensures a 0.1 nm wavelength resolution corresponding to a resolving power of about 1200 at 10 eV. This monochromator has been used for the recording of low-resolution absolute photoabsorption spectra in the 5-25 eV photon energy range. Its grating is most well suited for recording spectra above the 16 eV photon energy range.

The 3m-NIM-2 beam line at the BESSY II facility (Berlin, Germany) has been described by Reichardt et al. [14]. This 3m-NIM monochromator is positioned at a bending magnet frontend. It is equipped with two spherical gratings, i.e., an Al/MgF₂-grating of 600 lines mm^{-1} and a Pt-grating of 2400 lines mm^{-1} . The entrance and exit slits were adjusted between 10 μm and 40 μm leading to a resolving power of about 25,000 to 13,000 at 10 eV (124 nm) photon energy. This monochromator was used for recording high resolution spectra in the low photon energy range between 6 eV and 16 eV. Most of the spectra discussed in the present work were measured with 40 μm entrance and 10 μm exit slits and using the 600 l/mm Al/MgF₂-grating.

In all above described setups, the light has to pass through a 1 mm thick stainless steel microchannel plate at the exit slit of the monochromator in order to maintain a differential pressure of 1:1000 before entering a 30 cm long stainless steel absorption cell. The vapor pressure in the cell is measured by a Balzers capacitor

manometer. The light is detected by a sodium salicylate sensitized photomultiplier located at the end of the absorption cell in front of the absorption cell entrance slit. Output pulses are recorded by a 100 MHz counter. The recording of an absorption spectrum requires one scan with gas in the absorption cell and one with the evacuated cell. The stability of the synchrotron radiation and of the pressure in the cell ensured reliable absorption data. If necessary, the spectra presented in the following sections are corrected for any pressure drift.

We recently reported on the threshold photoelectron spectroscopy of 1,1-C₂H₂F₂ [3] using a second 3m-NIM monochromator equipped with a Pt grating of 2400 lines mm⁻¹. The threshold photoelectron current had to be normalized to the monochromator transmission function. For this purpose the photoelectron current generated by a gold diode located in front of the exit slit is measured. This latter signal can be normalized to the diode current measured with the evacuated ionization chamber. As a result, a log₁₀[*I*₀/*I*]-curve as a function of the photon energy, that is, a non-calibrated photoabsorption spectrum recorded with a non-calibrated detector is obtained. These kinds of experiments have been described earlier [2] and will be referred to in Section 3. In this curve, below 12 eV, the diode signal has to be assigned to the photoionization of Au. The photoelectron spectrum of gas phase Au shows, above the threshold at 9.22 eV, doublets at 11.1-11.4 eV and at 12.6-12.9 eV corresponding to the ³D and ¹D states of Au⁺ [15]. In the solid state, the latter is likely hidden in the broad band at 12.14 eV corresponding to an absorption band of C₂H₂F₂ and the former gives a broadened band near 11.19 eV. No signal due to Au has been reported above 13 eV.

The sample pressure has been maintained at 35-38 μbar to avoid saturation. The commercially available 1,1-C₂H₂F₂, purchased from Fluochem Ltd. and of 99.5% purity, was used without further purification.

2.2. Data handling and error estimation

As will be mentioned in the next sections, weak sharp peaks and diffuse structures are often superimposed on a strong continuum. To make the characterization of these features easier, a continuum subtraction procedure has been applied. This method has already been used successfully in previous spectral analyses [16]. For this purpose, the experimental curve is strongly smoothed to simulate the underlying continuum which is then subtracted from the original photoabsorption spectrum. The smoothing procedure consists in filtering the experimental curve by fast Fourier transform (FFT). The weak features emerge from a remaining strongly attenuated background. The resulting diagram will be called Δ-plot in the forthcoming sections. To verify that no weak structure has been removed by this operation, the same procedure is applied to the subtracted continuum. The result is a signal oscillating about zero with amplitudes of about two orders of magnitude or even lower than the signal resulting from the first operation. This has been demonstrated by Marmet [17] and Carbonneau [18].

The wavelength calibration of the 1.5m-NIM monochromator has been performed by using the Ar absorption spectrum between the ²P_{3/2} and the ²P_{1/2} ionic states. The accuracy of this calibration is better than 2 meV. In the measurements between 10 eV and 25 eV photon energy, the photoabsorption spectrum has been recorded with an energy interval of about 4 meV. The error on the energy position of a feature is estimated to be 6 meV. In the photoabsorption spectra between 5 eV and 11 eV, an energy increment of 1 meV has been adopted. The error on the energy position of a feature is estimated to be of the order of 3 meV. This evaluation is confirmed by the reproducibility of energy positions measured in different spectra recorded over several years.

3. Experimental results

The vacuum UV photoabsorption spectrum (PAS) of 1,1-C₂H₂F₂ as measured between 5 eV and 25 eV photon energy is shown in Fig. 1. The good control of the experimental parameters allows us to display the spectrum in terms of the molecular extinction coefficient $\epsilon_{m\nu}$ as a function of the photon energy (eV). For comparison above 10 eV, the gold diode signal (see discussion in Section 2.1) as normalized to the 13 eV extinction coefficient and measured with the 3 m-NIM monochromator at the BESSY I facility is also displayed. As clearly observed in this figure the transmission of the gold plated grating rapidly decreases above 22 eV giving rise to a rapid degradation of the signal-to-noise ratio. For clarity in the following discussion and as represented in Fig. 1 the PAS will be divided into three parts.

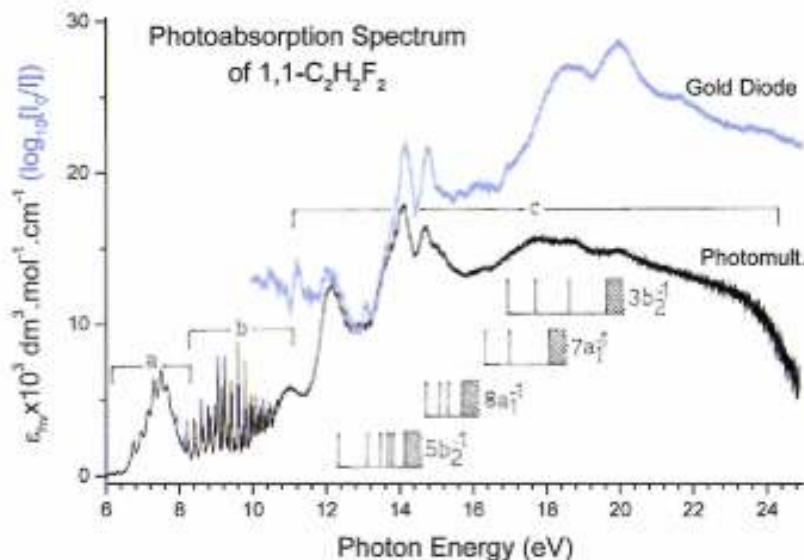
(a) The low-energy part extending between 6 eV and 8.2 eV corresponds to a single broad structured peak and it is reproduced in Fig. 2(a). The energy increment is of 1 meV. Vertical bars locate the structures and their energy positions are gathered in Table 1. Fig. 2(b) shows the result of the treatment of the peak by the subtraction method (see Section 2.2). For discussion purposes, the shifted HeI photoelectron spectrum (PES) of the first photoelectron band of 1,1-C₂H₂F₂ [3] is superimposed on this Δ-plot.

(b) The crowded PAS region between 8.2 eV and 11.2 eV consists of numerous sharp and strong to very weak peaks. This part of the PAS is represented in Fig. 3(a)-(c) on an expanded photon energy scale and the energy increment is 1 meV. The photoabsorption spectrum in this energy range is represented in terms of the extinction coefficient: owing to the intensity and sharpness of the features, the subtraction procedure was not really necessary here and has therefore not been applied. Vertical bars indicate the energy position of the observed features and these are gathered into different groups corresponding to vibrational progressions as listed in Table 2. The Rydberg series analysis of this energy region is shown in Table 3. To avoid overcrowding the Rydberg series have not been represented in Fig. 3.

(c) A wide photon energy region extending between 11 eV and 25 eV consists mainly of several broad and structureless bands and a few vibrational structures. A part of this area, recorded with 2 meV increments, is reproduced in Fig. 4 (a). In Table 4 we list the energy position of the structures observed in this energy range.

Fig. 4(b) shows the Δ -plot resulting from the subtraction method applied to this region of the PAS. A tentative simulated spectrum has been superimposed to this plot. Owing to the weakness and the diffuseness of the structures observed in the photon energy range of 12-14 eV, this spectral region has been recorded several times over several years under various experimental conditions. The energy positions and the relative intensities are very reproducible. Obviously, the energy position of these structures is easier to measure in such a diagram.

Fig. 1. VUV photoabsorption spectrum (black) of 1,1-C₂H₂F₂ between 6 eV and 25 eV photon energy. Horizontal bars (a), (b) and (c) indicate the three energy ranges analyzed in this work. The high energy part of the photoabsorption spectrum (blue) as measured using a gold diode as a light detector is included. This latter signal has been normalized to the extinction at 13 eV photon energy. Vertical bars and shaded areas locate Rydberg states and their convergence limit (or ionization continua). (For interpretation of the references to color in this figure legend, the reader is referred to the web version of this article.)



4. Discussion of the experimental data

The molecular orbital configuration of 1,1-C₂H₂F₂ in the C_{2v} symmetry group is described by

$$F(1b_2^2 1a_1^2) - C(2a_1^2 3a_1^2)$$

$$4a_1^2 2b_2^2 5a_1^2 6a_1^2 3b_2^2 1b_1^2 7a_1^2 1a_2^2 4b_2^2 8a_1^2 5b_2^2 2b_1^2: \tilde{X}^1 A_1$$

where the 4a₁ and 2b₂ are the inner-valence shell orbitals on F, the other orbitals being outer-valence shell orbitals. The 2b₁ MO has a predominant π character.

We measured the high resolution HeI-PES and threshold photoelectron spectra (TPES) of 1,1-C₂H₂F₂ and the results have been reported recently [3]. The first adiabatic ionization energy IE_{ad}(1,1-C₂H₂F₂⁺, X²B₁) is equal to (10.298 ± 0.001) eV. The corresponding vertical value IE_{vert}(1,1-C₂H₂F₂⁺, X²B₁) is equal to (10.688 ± 0.001) eV. These values are in very good agreement with earlier determinations as discussed in a recent report [3].

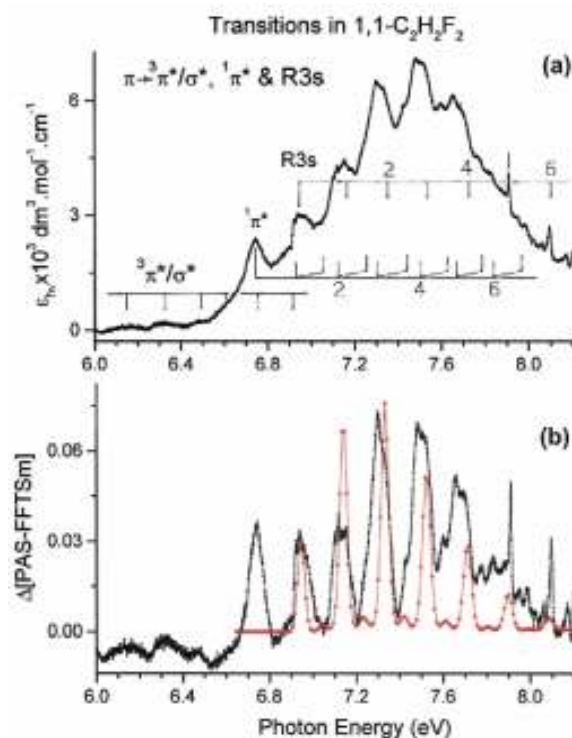
At higher energies four bands are observed by HeI-PES and were characterized by their vertical ionization energies at 14.810 eV, 15.716 eV, 18.157 eV and 19.820 eV [3]. In the TPES measured between 10 eV and 30 eV two maxima are observed at energies above the 21.22 eV limit [3], i.e. at 21.398 eV and 24.05 eV successively.

4.1. The valence and 3s Rydberg transitions (see Figs. 2 and 5)

This photon energy range is represented in Fig. 1 by range (a).

The typical ethylenic broad band is observed in 1,1-C₂H₂F₂ with a maximum at 7.52 eV. Contrary to the observations made in the PAS of C₂H₄ and C₂H₃F [1], the vibrational structure consists essentially of broad but structured peaks. Only the first broad peak at 6.742 eV seems to be structureless and on the high energy side of the major band two weak but sharp features appear, having the characteristic aspect of Rydberg transitions. The comparison of the same band in three different related compounds, i.e. C₂H₄, C₂H₃F [1] and 1,1-C₂H₂F₂, as investigated in the present work, is very informative as shown in Fig. 5(a) where the different contributions of valence and Rydberg transitions have been included.

Fig. 2. VUV photoabsorption spectrum of 1,1-C₂H₂F₂ between 6 eV and 8.2 eV photon energy: (a) molecular extinction coefficient ϵ_{ν} ; vertical bars show the valence (V) $\pi(2b_1) \rightarrow v(^1\pi^*, ^3\pi^*)$ and the transitions to the 3s Rydberg series. Only the even quanta v are indicated, (b) Δ -plot as a function of the photon energy (eV); the first band of the HeI-PES of 1,1-C₂H₂F₂ is inserted.



Comparing the three compounds, the measurement of the peak maximum is not very significant because of the important changes of the fine structure in each band. More valuable is the measured or estimated adiabatic excitation energy. As shown in Fig. 5(b) the $\pi \rightarrow 3s$ Rydberg transition shows a red shift when the substituting halogen atom becomes heavier, i.e. in the order H > F > Cl > Br as resulting from our previous investigations

Fig. 3. VUV photoabsorption spectrum of 1,1-C₂H₂F₂ on an expanded photon energy scale between 8.0 eV and 11.2 eV: (a) from 8.0 eV to 9.2 eV, (b) from 9.0 eV to 10.2 eV and (c) 10.0 eV to 11.2 eV. Long vertical bars indicate the vibrationless (0,0) transitions of the indicated Rydberg transitions. For each transition, the vibrational progression(s) are drawn using short vertical bars and only the even quanta v are marked. The shaded area corresponds to the convergence limit at the first adiabatic ionization energy of 1,1-C₂H₂F₂ at 10.298 eV [3].

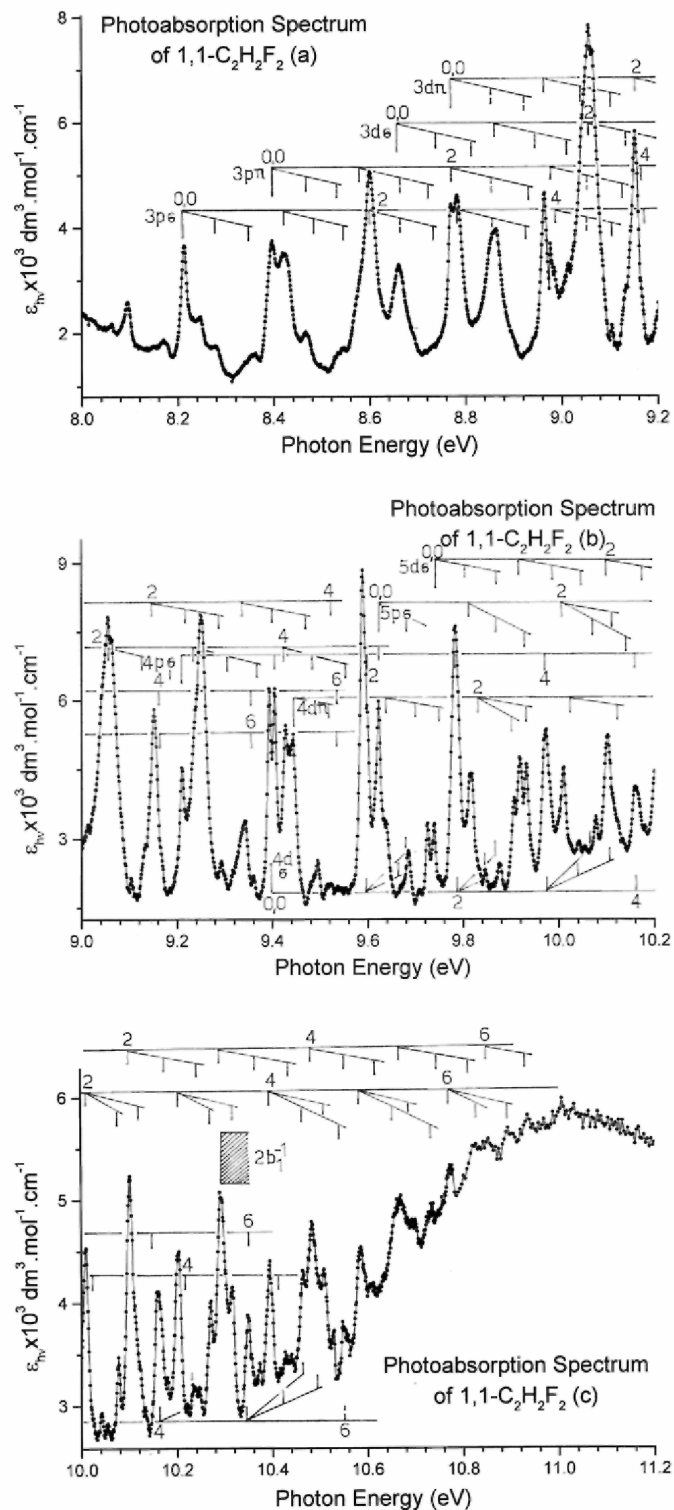
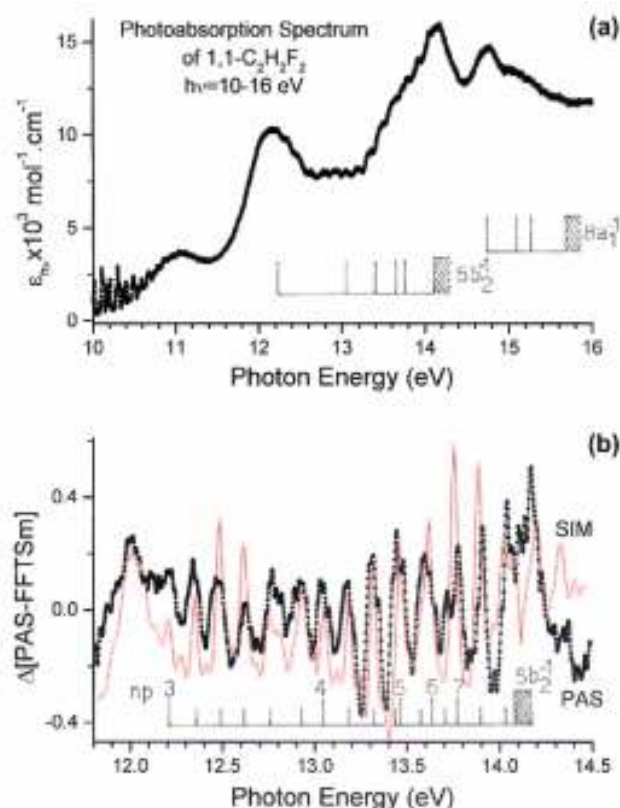


Fig. 4. VUV photoabsorption spectrum of 1,1-C₂H₂F₂ on an expanded photon energy scale between 10.0 eV and 16.0 eV (a) showing the weak vibrational structures, (b) corresponding Δ -plot (PAS) between 11.8 eV and 14.5 eV showing the detail of the vibrational structure. The simulated (SIM) spectrum is also displayed and the vibrational analysis is indicated by vertical bars.



[1,13,20]. As shown in the same figure the $\pi \rightarrow \pi^*(V)$ transition exhibits a much larger red shift. Owing to the resulting smaller overlap of the $\pi^*(V)$ and the 3sR states, the Valence-to-Rydberg interaction invoked for the interpretation of the 7.6 eV peak in C₂H₄ is expected to decrease following the same sequence.

With these observations and considering the first peak at 6.742 eV in the 7.52 eV band in 1,1-C₂H₂F₂, we assigned it to the adiabatic excitation energy of the $\pi(2b_1) \rightarrow \pi^*(V)$ transition. This assignment fits in the trend of the red shift of the adiabatic excitation energy of the $\pi \rightarrow \pi^*(V)$ transition by increasing the number of identical substituting atoms C₂H₄ > C₂H₃F > 1,1-C₂H₂F₂ (see Fig. 5(a)). Table 1 and Fig. 2 show the vibrational analysis of the excited $\pi^*(V)$ state. Essentially one vibrational progression is detected with $hc\omega_1 = 183 \pm 10$ meV (1475 ± 80 cm⁻¹). This vibration is combined with one quantum of a vibrational mode with $hc\omega_2 = 121 \pm 3$ meV (976 ± 24 cm⁻¹).

In order to assign these two energies to clearly identified vibrational modes of the excited molecule, we have to compare them with those observed for the ground states of the neutral [21] and the cation [3]. As a result, three wavenumbers have to be considered: 1730 cm⁻¹, 1354 cm⁻¹ and 916 cm⁻¹ in the case of the neutral molecule and 1573 cm⁻¹, 1438 cm⁻¹ and 895 cm⁻¹ in the cation and corresponding for both species to ν_2 (C=C stretching), ν_3 (H-C-H bending) and ν_4 (C-F and C=C stretching). Considering the MO involved in the excitation, the wavenumber of 1475 ± 80 cm⁻¹ is assigned to ν_2 whereas 976 ± 24 cm⁻¹ could unambiguously be assigned to ν_4 on the basis of the same argument. The assignments are listed in Table 1.

The two weak but sharp structures at 7.909 eV and 8.095 eV located at the end of the vibrational progression of the $(2b_1)^1(\pi^*)^1$ state appear as typical Rydberg transitions. Their assignment to the $2b_1 \rightarrow 3p$ transition [4,7] is discarded. This type of transition is usually much stronger if not one of the strongest transitions in the vacuum UV-PAS. As already suggested earlier [2], it can reasonably be assumed that the geometry of states belonging to a given Rydberg series is close to that of the cationic state to which it converges. This implies that its vibrational structure is expected to be close to that of the cation. This similarity could be helpful to

disentangle the vibrational fine structure belonging to the $\pi(2b_1) \rightarrow 3s$ transition. To make the comparison easier the Δ -plot of the appropriate PAS energy range will be compared to the HeI-PES of the $1,1\text{-C}_2\text{H}_2\text{F}_2^+(\tilde{X}^2B_1)$ state as measured in our laboratory [3]. The result is shown in Fig. 2(b) which not only enhances the weak structures but also the structures in each separate peak. Obviously the first peak is structureless.

Table 1 Energy position (eV), wavenumber (cm^{-1}) and assignments proposed for the vibrational structure observed in the vacuum UV photoabsorption spectrum of $1,1\text{-C}_2\text{H}_2\text{F}_2$ between 6.0 eV and 8.2 eV. Comparison is made with the results and assignments of [7] ($1 \text{ eV} = 8\,065.545 \text{ cm}^{-1}$ [19]).

This work			[7]	
Energy (eV)	Wavenbr. (cm^{-1})	Assignment	Energy (eV)	Assignment
6.157	49660	$V(\sigma^*/\pi^*)v$	-	-
6.318	50958	$V(v+1)$	-	-
6.471	52192	$V(v+2)$	-	-
6.622	53208	$V(v+3)$	-	-
6.742	54378	$V^+(\pi^*)(0,0)$	6.747	R3s(0,0)
6.902	55596	$V(v+5)$	6.882	R3s, v_8
6.939	55967	V', v_2	6.936	R3s, v_2
6.957	56112	R3s(0,0)	6.971	R3s, $v_4 + v_8$
7.024	56652	na	-	-
7.057	56918	$V', v_2 + v_4$	7.059	R3s, $v_2 + v_8$
7.116	57394	$V', 2v_2$	7.124	R3s, $2v_2$
7.152	57685	R3s, v_2	7.154	R3s, $v_2 + v_4 + v_8$
7.189	57983	na	-	-
7.238	58378	$V', 2v_2 + v_4$	7.240	R3s, $2v_2 + v_8$
7.300	58878	$V', 3v_2$	7.308	R3s, $3v_2$
7.332	59136	R3s, $2v_2$	7.336	R3s, $2v_2 + v_4 + v_8$
7.426	59895	$V', 3v_2 + v_4$	7.424	R3s, $3v_2 + v_8$
7.482	60346	$V', 4v_2$	7.485	R3s, $4v_2$
7.517	60629	R3s, $3v_2$	7.514	R3s, $3v_2 + v_4 + v_8$
7.602	61314	$V', 4v_2 + v_4$	7.599	R3s, $4v_2 + v_8$
7.656	61750	$V', 5v_2$	7.656	R3s, $5v_2$
7.693	62048	R3s, $4v_2$	7.706	R3s, $4v_2 + v_4 + v_8$
7.774	62702	$V', 5v_2 + v_4$	7.764	R3s, $5v_2 + v_8$
7.828	63137	$V', 6v_2$	7.832	R3s, $6v_2$
-	-	-	7.867	R3s, $5v_2 + v_4 + v_8$
7.909	63790	R3s, $5v_2$	7.912	R3p, (0,0)
7.950	64121	$V', 6v_2 + v_4$	7.950	R3s, $6v_2 + v_8$
7.986	64411	R3s, $5v_2 + v_A$	7.984	R3p, v_4
8.023	64710	$V', 7v_2$	8.025	R3s, $7v_2$
-	-	-	8.046	R3s, $6v_2 + v_4 + v_8$
8.061	65016	R3s, $5v_2 + 2v_A$	8.064	R3p, $2v_4$
8.095	65291	R3s, $6v_2$	8.096	R3p, v_2

Beside the $\pi \rightarrow \pi^*$ transition and its vibrational excitation, obviously another vibrational progression is present in the 7.52 eV band. Fitting the HeI-PES on the last narrow peaks, the result of this comparison is displayed in Fig. 2(b). The position in energy of the structures is drawn in Fig. 2(a) and the values are listed in Table 1. From this procedure an adiabatic excitation energy $EE_{\text{ad}} = 6.957 \text{ eV}$ is deduced and assigned to the 3s Rydberg transition, instead of the value 6.747 eV reported previously [4,7]. The energy onset at 6.742 eV measured in the present work is assigned to the $EE_{\text{ad}}(\pi^*)$ state. Furthermore, the major vibrational progression in the Rydberg transition is characterized by a wavenumber $\omega_2 = 1532 \pm 80 \text{ cm}^{-1}$ ($190 \pm 10 \text{ meV}$) which is assigned to the C=C, C-F stretching vibration [3]. As shown in Fig. 2 and in Table 1 in the last part of the band a few very weak structures could be ascribed to a smaller wavenumber $\omega_A \approx 605 \text{ cm}^{-1}$ (75 meV) which is compatible with the v_5 vibration characterized by $\omega_5 = 532 \pm 56 \text{ cm}^{-1}$ [3] in the cation and 544 cm^{-1} [21] in the neutral molecule. The increase of v_2 from 1475 cm^{-1} in the π^* state to 1532 cm^{-1} in the 3s-Rydberg state is related to the transition to an antibonding π^* MO and to a virtual 3s MO respectively.

Below 6.747 eV a very weak wavy background signal is detected. This structure does not appear in the

spectrum as reported by Limao-Vieira et al. [7], even though the signal-to-noise ratio is comparable. Different experimental conditions, in particular a lower transmission of the monochromator in this energy range, could account for this discrepancy. It should be emphasized that corresponding bands appear also with increasing intensity and blue shifted in other ethylene derivatives [22]. Furthermore, to the best of our knowledge Dauber and Brith [5] and Coggiola et al. [8] are the only previous works reporting about absorption of 1,1-C₂H₂F₂ below 6.0 eV. Only the latter group clearly showed the existence, by electron energy loss spectroscopy, of an absorption band at 4.63 eV extending from 3.8 eV to 6.5 eV. It was assigned to a $\pi(2b_1) \rightarrow {}^3\pi^*(T)$ transition. A fine structure could be observed (see Fig. 5(a) in Ref. [8]) but has not been mentioned or discussed by the authors. Though forbidden, but owing to its very low intensity as observed in this work, such a transition could be involved between 6.157 eV and 6.902 eV. However, an alternative assignment would be a $\pi \rightarrow \sigma^*$ transition as observed [23] and predicted [24] in the C₂H₂Cl₂ isomers in about the same energy range.

As shown in Table 1, starting at 6.157 eV and up to 6.902 eV, five peaks are detected with a decreasing interval of about 161 meV to 144 meV. They could very likely be assigned to the ν_3 H-C-H bending normal mode which has a wavenumber of 1354 cm⁻¹ (168 meV) in the neutral molecule [21] and is not detected in the cation [3]. From the present data, this vibrational motion appears to be fairly anharmonic.

Valence (V)-Rydberg (R) mixing is expected between the π^* and the 3s states. However, the two types of structures showing up in Fig. 2 differ clearly by their respective widths and intensities. This is particularly obvious for the vibrational structures at 7.909 eV and at 8.095 eV. As in the case of the corresponding transition in C₂H₃F at 7.6 eV [1], we suggest that V/R mixing is in this case also (or even more) limited so that a usual vibrational analysis is possible. In other words, the expansions of the mixed states on the basis of the pure V and R states are each dominated by a leading term so that it is reasonable to speak about a "Rydberg-like" and a "Valence π^* -like" state.

Table 2 Energy position (eV), corresponding wavenumber (cm⁻¹) and assignments proposed in the present work for the structures detected in the vacuum UV photoabsorption spectrum of 1,1-C₂H₂F₂. In the fourth column the averaged value of the energy and wavenumber associated with each proposed vibrational mode is indicated. Comparison is made only with the results of Ref. [7]. Conversion factor 1 eV = 8 065.545 eV [19].

This work			[7]
Energy (eV) ^a	Wavenbr. (cm ⁻¹)	Assignments	Energy (eV)
2b₁ → 3pσ			
8.213	66242	(0,0)	8.214
8.247	66517	na	8.246
8.279	66775	ν_5	8.279
8.306	66992	ν_4	-
8.355	67388	2 ν_5	8.358
8.421	67920	ν_2	8.423
8.493	68501	V2 + V5	8.504
8.545	68920	$\nu_2 + 2\nu_5$	8.548
8.600	69364	2ν_2	8.604
[8.660]	69 848	2 $\nu_2 + \nu_5$	8.664
8.733	70436	2 $\nu_2 + 2\nu_5$	-
8.782	70832	3ν_2	8.784
[8.858]	71445	3 $\nu_2 + \nu_5$	-
[8.929]	72017	3 $\nu_2 + 2\nu_5$	-
8.983	72453	4ν_2	-
[9.055]	73033	4 $\nu_2 + \nu_5$	9.063
[9.134]	73671	4 $\nu_2 + 2\nu_5$	-
[9.164]	73913	5ν_2	9.157
[9.360]	75494	6ν_2	9.364
[9.536]	76913	7ν_2	-
2b₁ → 3pπ			
8.396	67718	(0,0)	8.400
8.466	68283	ν_5	8.472
[8.493]	68501	ν_4	8.504
8.531	68807	2 ν_5	8.548
8.585	69243	ν_2	-
8.692	70106	$\nu_2 + \nu_4$	-
[8.733]	70436	$\nu_2 + 2\nu_5$	8.747

[8.769]	70727	2v₂	-	
8.865	71501	2v + v ₄	-	
[8.929]	72017	2v ₂ + 2v ₅	-	
8.975	72388	3v₂	8.965	
[9.055]	73033	3v ₂ + v ₅	-	
9.083	73299	3v + v ₄	-	
[9.134]	73671	3v ₂ + 2v ₅	-	
[9.164]	73913	4v₂	9.157	
[9.360]	75494	5v₂	9.364	
[9.536]	76913	6v₂	9.534	
2b₁ → 3dσ				
[8.660]	69848	(0,0)	8.664	$\omega_2 = 191 \pm 9 \text{ meV}$
[8.733]	70436	v ₅	8.747	$1541 \pm 72 \text{ cm}^{-1}$
8.819	71130	2v ₅	-	$\omega_5 = 72 \pm 9 \text{ meV}$
[8.858]	71445	v₂	8.866	$581 \pm 72 \text{ cm}^{-1}$
[8.929]	72017	v ₂ + v ₅	-	
9.013	72695	v ₂ + 2v ₅	-	
9.055	73034	2v₂	9.063	
[9.134]	73671	2v ₂ + v ₅	-	
9.194	74155	2v ₂ + 2v ₅	-	
9.249	74598	3v₂	9.256	
9.317	75147	3v ₂ + v ₅	9.329	
9.393	75760	3v ₂ + 2v ₅	-	
9.425	76018	4v₂	-	
9.494	76574	4v ₂ + v ₅	9.497	
9.568	77171	4v ₂ + 2v ₅	-	
9.621	77599	5v₂	-	
9.684	78107	5v ₂ + v ₅	9.690	
2b₁ → 3dπ				
[8.769]	70727	(0,0)	-	$\omega_2 = 192 \pm 2 \text{ meV}$
[8.858]	71445	v ₅	8.866	$1549 \pm 16 \text{ cm}^{-1}$
[8.929]	72017	2v ₅	-	$\omega_5 = 74 \pm 8 \text{ meV}$
8.963	72291	v₂	8.965	$597 \pm 64 \text{ cm}^{-1}$
9.044	72945	v ₂ + v ₅	9.030	
9.104	73429	v ₂ + 2v ₅	-	
9.152	73816	2v₂	9.157	
9.227	74421	2v ₂ + v ₅	9.215	
9.292	74945	2v ₂ + 2v ₅	9.298	
9.344	75364	3v₂	9.347	
9.416	75945	3v ₂ + v ₅	9.410	
[9.494]	76574	3v ₂ + 2v ₅	-	
9.536	76913	4v₂	9.534	
9.612	77526	4v ₅ + v ₅	-	
[9.684]	78107	4v ₂ + 2v ₅	9.690	
2b₁ → 4pσ				
9.210	74284	(0,0)	9.215	$\omega_2 = 190 \pm 4 \text{ meV}$
9.272	74784	v ₅	-	$1532 \pm 32 \text{ cm}^{-1}$
9.317	75147	v ₄	-	$\omega_4 = 102 \pm 7 \text{ meV}$
[9.360]	75494	2v ₅	9.364	$823 \pm 56 \text{ cm}^{-1}$
9.405	75856	v₂	9.400	$\omega_5 = 73 \pm 9 \text{ meV}$
9.480	76461	v ₂ + v ₅	-	$589 \pm 72 \text{ cm}^{-1}$
[9.513]	76728	v ₂ + v ₄	-	
9.554	77058	v ₂ + 2v ₅	-	
9.598	77413	2v₂	-	
9.670	77994	2v ₂ + v ₅	9.690	
9.707	78292	2v ₂ + v ₄	-	
9.750	78639	2v ₂ + 2v ₅	9.743	
[9.783]	78905	3v₂	9.786	
[9.846]	79413	3v ₂ + v ₅	9.852	
[9.876]	79655	3v ₂ + v ₄	-	

[9.932]	80107	$3v_2 + 2v_5$		9.939
9.972	80430	$4v_2$		9.979
[10.041]	80986	$4v_2 + v_5$		10.047/ 10.060
10.077	81276	$4v_2 + v_4$		10.084
[10.122]	81639	$4v_2 + 2v_5$		10.129
10.159	81938	$5v_2$		10.167
[10.235]	82551	$5v_2 + v_5$		10.242
10.302	83091	$5v_2 + 2v_5$		-
10.348	83462	$6v_2$		10.358
10.405	83922	$6v_2 + v_5$		10.401
10.450	84285	$6v_2 + v_4$		-
$2b_1 \rightarrow 4d\sigma$				
9.393	75760	(0,0)	$\omega_2 = 191 \pm 5 \text{ meV}$	-
9.459	76292	v_5	$1540 \pm 40 \text{ cm}^{-1}$	9.446
9.494	76575	v_4	$\omega_4 = 98 \pm 3 \text{ meV}$	-
9.536	76913	$2v_5$	$790 \pm 24 \text{ cm}^{-1}$	9.534
9.589	77341	v_2	$\omega_5 = 75 \pm 11 \text{ meV}$	9.596
9.649	77824	$v_2 + v_5$	$605 \pm 88 \text{ cm}^{-1}$	9.643
[9.684]	78107	$v_2 + v_4$		-
[9.739]	78550	$v_2 + 2v_5$		9.732
9.783	78905	$2v_2$		9.786
9.846	79413	$2v_2 + v_5$		9.852
[9.876]	79655	$2v_2 + v_4$		-
[9.932]	80107	$2v_2 + 2v_5$		9.939
9.978	80478	$3v_2$		9.979
[10.041]	80986	$3v_2 + v_5$		10.047/ 10.060
[10.077]	81276	$3v_2 + v_4$		10.084
10.133	81728	$3v_2 + 2v_5$		-
10.164	81978	$4v_2$		10.167
[10.235]	82551	$4v_2 + v_5$		10.242
10.265	82793	$4v_2 + v_4$		-
10.316	83204	$4v_2 + 2v_5$		-
10.350	83478	$5v_2$		10.358
[10.416]	84011	$5v_2 + v_5$		10.401
[10.450]	84285	$5v_2 + v_4$		-
10.496	84656	$5v_2 + 2v_5$		10.489
$2b_1 \rightarrow 4d\pi$				
9.443	76163	(0,0)	$\omega_2 = 195 \pm 4 \text{ meV}$	9.446
[9.513]	76728	v_5	$1611 \pm 32 \text{ cm}^{-1}$	
9.638	77736	v_2	$\omega_4 = 102 \pm 7 \text{ meV}$	9.643
9.707	78292	$v_2 + v_5$	$843 \pm 56 \text{ cm}^{-1}$	-
[9.783]	78905	$v_2 + 2v_5$	$\omega_5 = 75 \pm 8 \text{ meV}$	9.786
9.834	79317	$2v_2$	$605 \pm 64 \text{ cm}^{-1}$	-
9.907	79905	$2v_2 + v_5$		9.911
[9.932]	80107	$2v_2 + v_4$		9.939
10.022	80833	$3v_2$		10.015
[10.122]	81639	$3v_2 + v_4$		10.129
10.179	82099	$3v_2 + 2v_5$		-
10.220	82430	$4v_2$		10.209
10.293	83019	$4v_2 + v_5$		10.298
10.316	83204	$4v_2 + v_4$		10.319
10.372	83656	$4v_2 + 2v_5$		-
[10.416]	84011	$5v_2$		-
10.475	84487	$5v_2 + v_5$		10.472
10.529	84922	$5v_2 + v_4$		-
10.568	85237	$5v_2 + 2v_5$		-
$2b_1 \rightarrow 5p\sigma$				
9.622	77607	(0,0)	$\omega_2 = 192 \pm 3 \text{ meV}$	9.626
[9.684]	78107	v_5	$1549 \pm 24 \text{ cm}^{-1}$	-

9.817	79179	ν_2	$\omega_4 = 111 \pm 7 \text{ meV}$	9.821
9.956	80301	$\nu_2 + 2\nu_5$	$895 \pm 56 \text{ cm}^{-1}$	-
10.010	80736	$2\nu_2$	$\omega_5 = 72 \pm 9 \text{ meV}$	10.015
10.077	81276	$2\nu_2 + \nu_5$	$581 \pm 72 \text{ cm}^{-1}$	10.084
[10.122]	81639	$2\nu_2 + \nu_4$		10.129
10.164	81978	$2\nu_2 + 2\nu_5$		10.167
10.200	82269	$3\nu_2$		-
10.271	82841	$3\nu_2 + \nu_5$		10.276
10.302	83091	$3\nu_2 + \nu_4$		10.298
10.355	83519	$3\nu_2 + 2\nu_5$		10.358
10.394	83833	$4\nu_2$		10.401
10.463	84390	$4\nu_2 + \nu_5$		10.472
10.508	84753	$4\nu_2 + \nu_4$		10.512
10.542	85027	$4\nu_2 + 2\nu_5$		10.547
10.584	85366	$5\nu_2$		10.592
10.654	85930	$5\nu_2 + \nu_5$		-
10.692	86237	$5\nu_2 + \nu_4$		10.702
10.733	86567	$5\nu_2 + 2\nu_5$		-
10.772	86882	$6\nu_2$		-
10.826	87318	$6\nu_2 + \nu_5$		-
10.894	87866	$6\nu_2 + \nu_4$		-
10.935	88197	$(7\nu_2)$		-
$2b_1 \rightarrow 5d\sigma$				
9.724	78429	(0,0)	$\omega_2 = 188 \pm 4 \text{ meV}$	9.732
[9.876]	79655	$2\nu_5$	$1516 \pm 32 \text{ cm}^{-1}$	-
9.918	79994	ν_2	$\omega_4 = 110 \pm 10 \text{ meV}$	9.911
10.000	80655	$\nu_2 + \nu_5$	$887 \pm 80 \text{ cm}^{-1}$	-
10.054	81091	$\nu_2 + 2\nu_5$	$\omega_5 = 74 \pm 8 \text{ meV}$	10.060
10.102	81478	$2\nu_2$	$597 \pm 64 \text{ cm}^{-1}$	10.105
10.179	82099	$2\nu_2 + \nu_5$		-
10.204	82301	$2\nu_2 + \nu_4$		-
10.246	82640	$2\nu_2 + 2\nu_5$		-
10.290	82994	$3\nu_2$		10.298
10.372	83656	$3\nu_2 + \nu_5$		-
10.399	83874	$3\nu_2 + \nu_4$		10.401
10.439	84196	$3\nu_2 + 2\nu_5$		10.432
10.482	84543	$4\nu_2$		10.489
10.547	85067	$4\nu_2 + \nu_5$		10.547
10.607	85551	$4\nu_2 + \nu_4$		-
10.632	85753	$4\nu_2 + 2\nu_5$		-
10.669	86051	$5\nu_2$		10.675
10.748	86688	$5\nu_2 + \nu_5$		10.744
10.772	86882	$5\nu_2 + \nu_4$		-
10.853	87535	$6\nu_2$		-
11.006	88769	$6\nu_2 + 2\nu_5$		-

^a Energy positions represented twice or more are given in square brackets.

As shown in Table 1, if the experimental results of the present work agree within the estimated error limits with those reported by Limao-Vieira et al. [7] their interpretation is quite different. These authors assigned the entire absorption band at 7.5 eV to the $\pi(2b_1) \rightarrow \pi^*(V)$ transition only. The vibrational structure [7] is assigned to a long ν_2 (C=C stretching) progression with an averaged wavenumber of $1476 \pm 64 \text{ cm}^{-1}$ ($183 \pm 8 \text{ meV}$) combined with either the ν_4 normal mode at $782 \pm 48 \text{ cm}^{-1}$ ($97 \pm 6 \text{ meV}$) or with a combination of ν_4 and ν_8 with $\omega_8 = 960 \pm 64 \text{ cm}^{-1}$ ($119 \pm 8 \text{ meV}$).

The wavenumber of $1476 \pm 64 \text{ cm}^{-1}$ for ν_2 [7] is in excellent agreement with the value at $1475 \pm 80 \text{ cm}^{-1}$ determined in the present work. Though the wavenumber of $960 \pm 64 \text{ cm}^{-1}$ [7] is in good agreement with $976 \pm 24 \text{ cm}^{-1}$ obtained in the present work, we assigned it to ν_4 instead of ν_8 [7] mainly for two convergent reasons: the ν_4 mode (i) involves the C-F and C=C stretching as expected in a $\pi(2b_1) \rightarrow \pi^*(V)$ excitation and (ii) it is a totally symmetric (a_1) mode whose excitation is allowed. Only those transitions involving even quantum numbers of the antisymmetric $\nu_8(b_2)$ mode would be allowed. Furthermore, in the present work, no evidence is found for the

wavenumber at $782 \pm 48 \text{ cm}^{-1}$ but a few observations which can be related with a wavenumber of $\omega_A \approx 605 \text{ cm}^{-1}$ (75 meV) have been mentioned above and were assigned to ν_5 which has a_1 symmetry.

Table 3 Rydberg series analysis of the vacuum UV photoabsorption spectrum of 1,1-C₂H₂F₂. Energy position (eV), corresponding wavenumber (cm⁻¹), effective quantum numbers (n*) and assignments proposed in this work. Comparison is made with the literature data [4,7]. Conversion factor 1 eV = 8065.545 eV [19].

This work			[4] (cm ⁻¹)	[7](eV)
eV	cm ⁻¹	n*		
<i>2b₁ → ns</i>				
6.957	55838	2.017	54348	6.747
8.799	70969	3.012	69930	8.784
9.455	76260	4.015	75821	9.446
9.750	78639	4.978	78585	9.786
9.932	80107	6.088	80064	9.939
-	-	-	80782	10.047
-	-	-	81334	10.105
-	-	-	81699	-
<i>2b₁ → npσ</i>				
8.213	66242	2.533	63776	7.912
9.210	72284	3.536	74344	9.157
9.622	77607	4.480	76670	9.626
9.846	79413	5.480	79397	9.852
9.973	80438	6.460	80483	9.979
-	-	-	-	10.060
<i>2b₁ → npπ</i>				
8.396	67718	2.674	-	-
9.295	74969	3.681	-	-
9.685	78115	4.707	-	-
9.877	79663	5.678	-	-
9.997	80631	6.712	-	-
10.068	81204	7.674	-	-
<i>2b₁ → ndσ</i>				
8.660	69849	2.882	70786	8.604
9.393	75760	3.875	76249	9.400
9.724	78429	4.868	78505	9.732
9.907	79905	5.891	79981	9.911
10.009	80728	6.849	-	10.015
10.077	81276	7.829	-	10.084
-	-	-	-	-
-	-	-	-	10.167
<i>2b₁ → ndπ</i>				
8.769	70727	2.982	-	8.866
9.443	76163	3.987	-	9.497
9.739	78550	4.929	-	-
9.918	79994	5.926	-	-

4.2. The Rydberg transitions

As shown in Fig. 1 the high photon energy region ranging from 8.2 eV to 25.0 eV is clearly divided in two parts: (b) the low-energy range extending from 8.2 eV to 11.2 eV consisting of an abundant strong to weak very sharp fine structure (Fig. 3) and (c) the high-energy range spread from 11.2 eV to 25 eV made of fairly strong and broad bands with additional more or less regular fine structure (see Fig. 4).

The simplest model which can be tested to disentangle a complex spectrum as shown in Fig. 1, is to neglect the perturbations between Rydberg series, that is, to use the Rydberg formula (1) and fit it to the energy position E_{Ryd} of the features:

$$E_{\text{Ryd}} = \text{IE} - \frac{R}{(n - \delta)^2} = \text{IE} - \frac{R}{(n^*)^2} \quad (1)$$

where the R is the Rydberg constant $R = 13.606$ eV [19], δ is the quantum defect, n^* is the effective quantum number and IE is the ionization limit to which the considered Rydberg series converges.

The successive ionization energies IE to be used in this work have been defined earlier in this section and are inserted in Figs. 1, 3 and 4. The fine structure mostly observed in the low-energy part (b) of the spectrum will be assigned to vibrational excitation associated with the successive Rydberg series. Robin [25] made a critical and extensive review of the analyses of Rydberg transitions and proposed rules and guidelines for assignments.

4.2.1. Rydberg transitions between 8.2 eV and 11.2 eV (see Fig. 3(a)-(c))

This photon energy range is represented by the range (b) in Fig. 1 and could be directly compared to the spectral data of Limao-Vieira et al. [7] available on the website referred to in Ref. [20] with respect to the intensity and the spectral resolution.

4.2.1.1. Electronic transitions. The vibrationless Rydberg transitions observed for 1,1-C₂H₂F₂ between 8.2 eV and 11.2 eV are partly shown in Fig. 3(a-c). To avoid overcrowding of this figure the higher terms of the various Rydberg series are not represented. Therefore, the Rydberg transitions observed in the present work have been listed in Table 3 together with their quantum defects. In the same table two previous data sets are included for comparison [4,7]. Their assignments have been reproduced implicitly. As mentioned earlier (see Section 2.2) the estimated error on the measurements in the present spectrum is about 2 meV or 16 cm⁻¹. No error estimation is provided by Bélanger and Sandorfy [4] and by Limao-Vieira et al. [7]. For the assignments reported in the present work the adiabatic ionization energy value $\text{IE}_{\text{ad}}(1,1\text{-C}_2\text{H}_2\text{F}_2, \tilde{X}^2\text{B}_1) = (10.298 \pm 0.001)$ eV [3] has been used.

A first $2b_1 \rightarrow ns$ Rydberg series (corresponding to the nR series in [4]) is observed up to $n = 7$ with an average quantum defect $\delta = 0.98 \pm 0.04$. Bélanger and Sandorfy [4] reported $\delta = 0.90$, using $\text{IE}_{\text{ad}} = 10.300$ eV as reported by Lake and Thompson [26], and observed the series up to $n = 10$. Limao-Vieira et al. [7] deduced a quantum defect $\delta = 0.94 \pm 0.09$ as based on the same value of the convergence limit. Between the previous works and present one the main difference is the assignment of the $2b_1 \rightarrow 3s$ transition and discussed in the last part of Section 4.1.

Following the long $3s$ Rydberg series progression, the first relatively strong transition is observed at 8.213 eV. It has been assigned to the $2b_1 \rightarrow 3p$ Rydberg transition with an effective quantum number $n^* = 2.533$. On this basis a short series of Rydberg transitions has been observed up to $n = 7$ with an average quantum defect $\delta = 0.50 \pm 0.03$ close to the characteristic "atomic" value for the p-type Rydberg orbital. This δ value can be compared with the $\delta = 0.49$ determined for the nR' series transitions observed by Bélanger and Sandorfy [4]. Limao-Vieira et al. [7] observed a series of Rydberg transitions assigned to $2b_1 \rightarrow np\lambda$ up to $n = 8$ with an averaged value $\delta = 0.58 \pm 0.03$. In this series only the energy position of the last three members agree within the error limits with those measured in the present work because we adopted 8.213 eV as the vibrationless $2b_1 \rightarrow 3p$ transition.

Starting at 8.396 eV a second series of Rydberg transitions has been observed which are characterized by an averaged quantum defect $\delta = 0.31(3) \pm 0.01(6)$. The first member of this series has an effective quantum number $n^* = 2.674$. These values would point at a p-character of the involved Rydberg orbital with expected δ value ranging from 0.4 to 0.6 [25,27]. As the core contains less orbitals with π symmetry than with σ symmetry, it is reasonable to expect that π Rydberg orbitals interact less with the ionic core and are therefore characterized by a smaller quantum defect. On the basis of this argument we assigned this series to $2b_1 \rightarrow np\pi$ whereas the lower energy series is ascribed to $2b_1 \rightarrow np\sigma$ Rydberg transitions. This series of Rydberg transitions have not been mentioned in previous studies of the vacuum UV spectrum of 1,1-C₂H₂F₂. Such different p-type Rydberg transitions have been observed earlier in C₂H₃Br [13] and in the methyl monohalides CH₃X (X= Cl, Br and I) [28].

At 8.660 eV a new Rydberg series starts and is characterized by $n^* = 2.882$, i.e. by a low value of the quantum defect. This series is observed in this work up to $n = 8$ with an averaged quantum defect $\delta = 0.13 \pm 0.02$ which is a typical value for nd -type Rydberg transitions. This series should correspond to the nR'' Rydberg

Table 4 Energy position (eV), corresponding wavenumber (cm^{-1}) and assignments of the major features in the vacuum UV photoabsorption spectrum of 1,1- $\text{C}_2\text{H}_2\text{F}$ between 11.8 eV and 25 eV photon energy. Comparison is made with photoionization [6] and electron scattering [8] results. Conversion factor $1 \text{ eV} = 8065.545 \text{ eV}$ [19].

This work		Literature data (eV)		
(eV) ^a	(cm^{-1})	Assignment	[8]	[6]
12.134-	97867-	Vibrationally resolved structures	12.2(3p)-	12.3-
14.178	114353		13.8(5s)	13.9
14.786/[14.75]	119257	$8a_1 \rightarrow 4p$ ($n^* = 3.65$)	14.2(6s)	14.3
15.062	121483	Vibrationally resolved structures	14.7(3s)	14.9
15.296/[15.33]	123370	$8a_1 \rightarrow 6p$ ($n^* = 5.62$)		
16.31/[16.14]	131549	$7a_1 \rightarrow 3s$ ($n^* = 2.83$)		
1.694/[16.97]	136630	$\begin{cases} 7a_1 \rightarrow 4p(n^* = 3, 51) \\ 3b_2 \rightarrow 3s(n^* = 2.33) \end{cases}$		
[17.31]				
17.69/[17.72]	142679	$3b_2 \rightarrow 3p$ ($n^* = 2.61$)		17.7
18.69/[18.35]	150745	$3b_2 \rightarrow 4p$ ($n^* = 3.67$)		18.4
20.25/[20.05]	163328	$6a_1 \rightarrow 4p$ ($n^* = 3.45$)		20.25
[21.7]	[175022]	$[6a_1^{-1}]$		
23.7/[23.9]	191153	$5a_1 \rightarrow 4s$ ($n^* = 3.01$)		
12.134-14.178 eV photon energy region				
12.224	98593	$5b_2 \rightarrow 3p: (0,0)$	$n^* = 2.69$	
12.274	98996	v_5		
12.350	99609	v_3		
12.456	100464	$V_3 + V_5$		
12.484	100690	$2v_3$		
12.534	101093	$2v_3 + 2v_5$		
12.634	101900	$3v_3$		
12.662	102126	$2v_3 + 3v_5$		
12.694	102384	$3v_3 + v_5$		
12.780	103078	$4v_3$		
12.826	103449	$4v_3 + v_5$		
12.936	104336	$5v_3$		
12.982	104707	$5v_3 + v_5$		
13.084	105530	$6v_3$		
13.048	105239	$5b_2 \rightarrow 4p: (0,0)$	$n^* = 3.61$	
13.178	106288	v_3		
13.330	107514	$2v_3$		
13.490	108084	na		
13.454	108514	$5b_2 \rightarrow 5p: (0,0)$	$n^* = 4.64$	
13.606	109740	v_3		
13.728	110724	$2v_3$		
13.656	110143	$5b_2 \rightarrow 6p: (0,0)$	$n^* = 5.57$	
(13.788) ^b	111208	v_3		
13.920	112272	$2v_3$		
(13.788) ^b	111208	$5b_2 \rightarrow 7p: (0,0)$	$n^* = 6.71$	
13.822	111482	na		
13.844	111659	v_5		
13.892	112047	$2v_5$		
13.980	112756	na		
14.050	113321	$2v_3$		
14.178	114353	$3v_3$		
15.07-15.70 eV photon energy region				
15.07	121548	$8a_s \rightarrow 5p$ (0,0)	$n^* = 4.65$	
15.18	122435	v_4		
15.33	123645	$3v_4$		
15.58	128356	$4v_4$		
15.68	126306	$5v_4$		

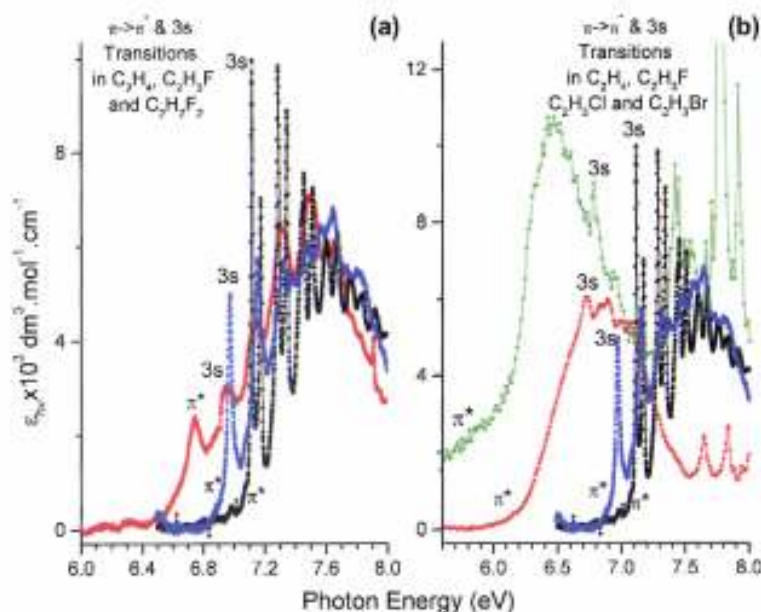
na: not assigned.

^a Positions in square brackets are measured in the "gold diode" photoabsorption spectrum: for explanation see text. ^b Value in parentheses: at least two possible assignments.

transitions in the work of Bélanger and Sandorfy [4] who reported a quantum defect $\delta = 0.2$ and observed the series up to $n = 6$.

Lima-Vieira et al. [7] mention two nd -type Rydberg transitions. The $nd\pi$ series starts at 8.604 eV and is observed up to $n = 10$ whereas an $nd\delta$ -type Rydberg series starts at 8.866 eV and is observed up to $n = 4$. For the former an averaged quantum defect $\delta = 0.20 \pm 0.05$ whereas for the latter an averaged $\delta \approx -0.08$ are reported [7]. In the present work clearly a Rydberg series is starting at 8.769 eV. Members of this nd series are observed up to $n = 6$ with an averaged quantum defect $\delta = 0.044 \pm 0.03$. This series is designated by $nd\pi$ whereas the former series starting at 8.660 eV by $nd\sigma$ by arguing that $nd\sigma$ should have a larger quantum defect than $nd\pi$ because the number of occupied σ orbitals in the core is larger than the number of π orbitals.

Fig. 5. The VUV photoabsorption spectra of (a) C_2H_4 , C_2H_3F and $1,1-C_2H_2F_2$ and (b) of C_2H_4 , C_2H_3F , C_2H_3Cl and C_2H_3Br on an expanded photon energy scale between 6.0 eV and 8.0 eV. The adiabatic excitation energies of the valence (π^*) and the Rydberg ($3s$) transitions are indicated for each molecule.



4.2.1.2. Vibrational analysis. Beside the vibrationless electronic transitions the majority of the most intense features in the $1,1-C_2H_2F_2$ PAS between 8.2 eV and 11.2 eV are not assigned. Owing to the n^{-3} intensity law the rather weak electronic members of higher principal quantum number n of the successive Rydberg series become difficult to detect. The vibrational transitions associated with the low n Rydberg states are characterized by a Franck-Condon distribution and can dominate the spectrum.

To disentangle this spectrum we shall rely on the assumption [25] that the vibrational structure of states belonging to Rydberg series is similar to that of the cationic state to which it converges. This hypothesis, which neglects perturbations due to Rydberg-Rydberg interactions, has been used successfully for the interpretation of the vacuum UV spectra of the methyl halides [28] and more recently of C_2H_3F [1]. The vibrationless convergence limit of all the Rydberg states involved between 8.2 eV and 11.2 eV is $IE_{ad}(1,1-C_2H_2F_2^+, \tilde{X}^2B_1) = (10.298 \pm 0.001)$ eV [3]. The cationic vibrational structure results from the excitation of three normal modes [3]. However, about 95% of the available intensity is distributed over the $C=C$ stretching mode ν_2^+ . Therefore, the HeI-PES band related to the \tilde{X}^2B_1 is "diatomic like" (see Fig. 2(b)). For the purpose of the decomposition of the PAS we use this HeI-PES spectrum which is translated and positioned with reference to the successive vibrationless Rydberg transitions.

The result of this procedure is represented in Fig. 3(a)-(c) and the energy positions and assignments are summarized in Table 2. In the same table the energy positions observed in the present work are compared to those reported by Lima-Vieira et al. [7]. For each Rydberg state the vibrational structure is assigned and the averaged values of the associated wavenumbers are tabulated.

Using this tool a first important confirmation is that the $2b_1 \rightarrow 3p$ Rydberg transition has to start at 8.213 eV as proposed in Section 4.2.1.1. The argument is that assuming that the transition starts at 7.912 eV as postulated in [4,7] leads to no correlation in either energy or intensity between the PAS and the HeI-PES. The same conclusion applies for the weak peak at 8.096 eV.

Except for the $2b_1 \rightarrow 3s$ Rydberg transition, for which a long v_2 progression is observed, no vibrational structure for higher ns -Rydberg members could be detected.

From the data displayed in Table 2 and related to the observed $np\lambda$ - ($n = 3-5$) and $nd\lambda$ - ($n = 3-5$) Rydberg states, mainly three vibrational modes are excited and their respective values are fairly constant within the standard deviations. The following assignments are proposed: $\nu_2 = 1549 \pm 16 \text{ cm}^{-1}$ (or $191 \pm 2 \text{ meV}$), $\nu_4 = 839 \pm 40 \text{ cm}^{-1}$ (or $104 \pm 5 \text{ meV}$) and $\nu_5 = 589 \pm 16 \text{ cm}^{-1}$ (or $73 \pm 2 \text{ meV}$) respectively. The indicated error limits represent the dispersion of the wavenumbers (or energies) over the nine Rydberg states. These values can be compared to those measured in the \tilde{X}^2B_1 state of the cation [3]: $\nu_2 = 1573 \pm 8 \text{ cm}^{-1}$, $\nu_4 = 895 \pm 16 \text{ cm}^{-1}$ and $\nu_5 = 532 \pm 56 \text{ cm}^{-1}$.

These values have to be compared with the vibrational analysis proposed by Limao-Vieira et al. [7], i.e. $hc\omega_2 = 184 \text{ meV}$ and a mode called $hc\omega_4 = 76 \pm 4 \text{ meV}$ in the 3p- and $70 \pm 10 \text{ meV}$ in 4p-Rydberg states. A ν_8 mode of $hc\omega_5 = 120 \text{ meV}$ in 3p and 117 meV in the 5p Rydberg state is determined. For the $nd\lambda$ -Rydberg states the $hc\omega_2$ vibrational energy lies in an interval of 191-194 meV which is in very good agreement with the value determined in the present work. Albeit assigning the wavenumbers at 66-77 meV and at about 112 meV to ν_4 and ν_8 respectively, these values correspond fairly well to $hc\omega_5 = 73 \text{ meV}$ (589 cm^{-1}) and $hc\omega_4 = 104 \text{ meV}$ (839 cm^{-1}) as assigned in the present work.

It has also to be mentioned that several energies are listed in Table 2 in square brackets meaning that the same signal has been assigned to several (at least two) energies. In many cases the discrepancy of local intensities between the reference PES spectrum and the PAS is accounted for by the sum of two or more overlapping contributions.

The fact that the experimental data could be satisfactorily analyzed using the simple Rydberg formula and assuming the same vibrational structure as in the corresponding ionic states indicates *a posteriori* that perturbations arising due to Rydberg-Rydberg or Rydberg-continuum interactions are small enough so that their influence on the energy positions could not be detected at the resolution reached in our spectra.

4.2.2. Rydberg transitions between 11.2 eV and 25.0 eV (see Figs. 1 and 4)

This photon energy range is represented in Fig. 1 by range (c). It consists of several strong bands with well defined maxima, shoulders and broad and weaker bands superimposed on a continuum of increasing intensity. The energy positions, assignments and comparison with literature values obtained by photoionization mass spectrometry [6] and electron impact spectroscopy [8] are listed in Table 4 and partly included in Fig. 1.

The PAS as observed in the photon energy range of 10-16 eV is represented in Fig. 4(a) on an expanded energy scale. Obviously this spectrum shows numerous substructures. A first rough picture using the maxima of the bands allows us to assign the structures between 12.224 eV and 13.454 eV to Rydberg states converging to the A^2B_2 ionic state at $IE_{ad} = 14.090 \pm 0.005 \text{ eV}$ [3] whereas at energies higher than 14.786 eV the convergence limit should be the B^2A_1 ionic state at $IE_{ad} = 15.40 \text{ eV}$ [3]. The effective quantum numbers are successively $n^* = 2.69, 3.61$ and 4.64 for the former group and 3.65 for the latter. These values clearly point to p-type Rydberg states. However, for the transition starting at 12.224 eV an effective quantum number $n^* = 2.007$ is also determined when the convergence limit at 15.4 eV [3] is considered. This hypothesis could not be discarded. The main argument pleading for the p-type Rydberg states is the fairly good convergence between the shifted photoelectron spectrum and the Δ -plot of the PAS (see Fig. 4(b)), as explained below.

In an attempt to interpret this part of the PAS, the subtraction method is applied in a first step (see Section 2.2). The resulting Δ -plot is obtained and shown in Fig. 4(b). In a second step the appropriate HeI-PES band of the cationic state is used, to which the considered Rydberg state(s) converge(s). As already mentioned earlier, the vibrationless transition of this "stencil" spectrum is translated to make it coincide with each vibrationless transition of the successive Rydberg states. The sum of these successive contributions could simulate qualitatively the Δ -plot. The result of this operation is shown in Fig. 4(b) and directly compared with the Δ -plot of the PAS. The reasonable qualitative agreement between the simulated (SIM) and the absorption spectrum (PAS) indicates that a $2b_2 \rightarrow np$ -Rydberg series ($n = 3-7$) is observed and converges to the A^2B_2 ionic

state of 1,1 - C₂H₂F₂⁺.

As in this spectral region medium intensity or weak structures are superimposed on a relatively intense continuum, Rydberg-ionization continuum interactions might be invoked, leading to Fano-profiles [29], which would make the subtraction procedure leading to the Δ -plots problematic. The large background results, however, from the contribution of many different ionization continua opened in this energy range and associated with the different electronic and vibrational ionic states. It is expected that all Rydberg states do not interact with the same strength with these various continua. In our work on the constant-ion-state (CIS) spectra [3], we observe that the latter show a similar shape for nearly all ionic states and are nearly structureless. Only the CIS-curves for the ground ionic state show a different behavior. We concluded by stating that only resonant (emission of zero-kinetic-energy electrons) is substantial in this system, so that a given Rydberg state interacts only with a very specific ionization continuum. High q -parameter and Lorentzian profiles are then expected.

On the other hand, from a technical data handling point of view now, it is very unlikely that the data handling procedure leading to the Δ -plots erases a Fano-profile. If a Fano-profile is present, the described procedure (see Section 2.2) which consists in obtaining a "pure" background by strongly smoothing the original spectrum should get rid, in this background and only in it, of the oscillations associated with medium q Fano-profiles. When this completely smoothed background is then subtracted from the original spectrum to enhance the present discrete structures, then the oscillations should reappear even more clearly, making the detection of Fano-profiles even more straightforward. Marmet [17] and Carbonneau [18] have highlighted Fano-profiles in this way many years ago. We are confident that Fano-profiles would have been highlighted in the Δ -plots, would they have been present in the original spectra.

The above mentioned procedure allowed us to analyze in detail the vibrational structure. The energy positions and the assignments are listed in Table 4. One vibrational wavenumber could be determined, i.e. $\omega_3 = 145 \pm 88 \text{ cm}^{-1}$ ($142 \pm 11 \text{ meV}$) in 3p, 1081 cm^{-1} (134 meV) in 4p and $1137 \pm 120 \text{ cm}^{-1}$ ($141 \pm 15 \text{ meV}$) in 5p Rydberg states. These values are close but higher than 1077 cm^{-1} (133 meV) determined for ν_3 in the A^2B_2 ionic state [3] where it corresponds to the H-C-H bending vibration. With less certainty, a second wavenumber is identified with $\omega_5 = 411 \pm 40 \text{ cm}^{-1}$ ($51 \pm 5 \text{ meV}$). It is comparable but lower than the value of $\omega_5 = 532 \text{ cm}^{-1}$ determined for the A^2B_2 ionic state [3] and has been assigned to an F-C-F bending vibration.

Using the same procedure between 15.07 eV and 15.70 eV a very weak structure is observed and assigned to vibrational excitation as shown in Table 4. The $8a_1 \rightarrow 5p$ Rydberg transition should be involved together with the excitation of the ν_4 vibrational mode with a wavenumber $\omega_4 \approx 970 \text{ cm}^{-1}$ which could be correlated with the value of $839 \pm 32 \text{ cm}^{-1}$ determined in the B^2A_1 excited state of the cation 1,1-C₂H₂F₂⁺ where it has been assigned to the C-F/C=C stretching [3].

Above 16 eV, the observed features could be assigned to Rydberg electronic transitions as shown in Table 4. The $7a_1 \rightarrow np$ and the $3b_2 \rightarrow np$ transitions dominate. This observation is in agreement with our earlier remark concerning the larger intensity of np -type with respect to ns -type transitions [1,13,28].

The features recorded in the absorbance spectrum obtained by using the gold diode detector agree fairly well with that observed using the photomultiplier. However, in the former the high energy bands are detected more efficiently, particularly above 18 eV. In this energy range Rydberg transitions from the $6a_1$ and $5a_1$ MO's may be involved.

5. Conclusions

The measurement of the VUV photoabsorption spectrum of 1,1-C₂H₂F₂ at improved resolution by using synchrotron radiation enabled us to extend for the first time the data above the 10.5 eV photon energy limit, i.e., from 10.5 eV to 25 eV. Contrarily to the usual broad and strong bands observed in the high energy range several peaks show vibrational structures for which assignments have been proposed.

Valence-valence ($2b_1 \rightarrow n^*$) as well as valence-Rydberg ($2b_1 \rightarrow 3s$) transitions are involved at the low energy part of the spectrum, i.e. between 6 eV and 8 eV. The vibrational structure has been interpreted in both states. A comparison is made with previous assignments proposed for the same transitions in C₂H₄, C₂H₃F [1], C₂H₃Cl [20] and C₂H₃Br [13].

In the 8.2-11.2 eV intermediate photon energy range, the abundant fine structure has been assigned to vibronic Rydberg transitions, i.e., $2b_1 \rightarrow ns$ ($n = 3-7$), $np\sigma$ and $np\pi$ ($n = 3-7$ and 3-8) and $nd\sigma$ and $nd\pi$ ($n = 3-8$

and 3-6) have been identified. All involved Rydberg states converge to the $1,1\text{-C}_2\text{H}_2\text{F}_2^+(\tilde{X}^2\text{B}_1)$ ground ionic state. The vibrational fine structure associated with these transitions has been analyzed based on the first band of the $1,1\text{-C}_2\text{H}_2\text{F}_2$ HeI-PES results [3]. This procedure allowed us to assign the observed structure to three vibrational modes (and their harmonics and combination) $\omega_2 = 1549\text{ cm}^{-1}$ (C=C and C-F stretching), $\omega_4 = 839\text{ cm}^{-1}$ (C-F symmetric stretch, C=C stretching) and $\omega_5 = 589\text{ cm}^{-1}$ (F-C-F bending).

Acknowledgments

We are indebted to the University of Liège, the Fonds de la Recherche Fondamentale Collective (FRFC) and the Freie Universität Berlin for financial support. R.L. and B.L. gratefully acknowledge the European Community for its support through its TMR (Contract EU-HPRI-1999CT-00028) and 13 (Contract R II 3 CT-2004-506008).

References

- [1] R. Locht, B. Leyh, D. Dehareng, H.W. Jochims, H. Baumgärtel, *Chem. Phys.* 362 (2009) 97.
- [2] R. Locht, B. Leyh, D. Dehareng, K. Hottmann, H. Baumgärtel, *J. Phys. B* 43 (2010) 015102.
- [3] R. Locht, D. Dehareng, B. Leyh, *J. Phys. B* 45 (2012) 115101.
- [4] G. Bélanger, C. Sandorfy, *J. Chem. Phys.* 55 (1971) 2055.
- [5] P. Dauber, M. Brith, *Chem. Phys.* 11 (1975) 143.
- [6] D. Reinke, R. Krässig, H. Baumgärtel, *Z. Naturf.* 28a (1973) 1021; D. Reinke, H. Baumgärtel, T. Cvitas, L. Klasinc, H. Glisten, *Ber. Bunsen Gesell. Phys. Chem.* 78 (1974) 1145.
- [7] P. Limao-Vieira, E. Vasekova, B.N. Raja Sekhar, N.J. Mason, S.V. Hoffmann, *Phys. Chem. Chem. Phys.* 8 (2006) 4766.
- [8] M.J. Coggiola, W.M. Flicker, O.A. Mosher, A. Kuppermann, *J. Chem. Phys.* 65 (1976) 2655.
- [9] S. Arulmozhiraja, M. Ehara, H. Nakatsuji, *J. Chem. Phys.* 126 (2007) 044306.
- [10] J. Gonzalez-Vazquez, L. Gonzalez, *Chem. Phys.* 349 (2008) 287.
- [11] F. Güthe, R. Locht, B. Leyh, H. Baumgärtel, K.M. Weitzel, *J. Phys. Chem. A* 103 (1999) 8404.
- [12] E. Gridelet, D. Dehareng, R. Locht, A.J. Lorquet, J.C. Lorquet, B. Leyh, *J. Phys. Chem. A* 109 (2005) 8225.
- [13] A. Hoxha, R. Locht, B. Leyh, D. Dehareng, K. Hottmann, H.W. Jochims, H. Baumgärtel, *Chem. Phys.* 260 (2000) 237.
- [14] G. Reichardt, T. Noll, I. Packe, P. Rotter, J.-S. Schmidt, W. Gudat, *Nucl. Instr. Methods A* 467-468 (2001) 458.
- [15] J.M. Dyke, N.K. Fayad, A. Morris, I.R. Trickle, *J. Phys. B* 12 (1979) 2985.
- [16] R. Locht, B. Leyh, A. Hoxha, D. Dehareng, H.W. Jochims, H. Baumgärtel, *Chem. Phys.* 257 (2000) 283.
- [17] P. Marmet, *Rev. Sci. Instrum.* 50 (1979) 79.
- [18] R. Carbonneau, E. Bolduc, P. Marmet, *Can. J. Phys.* 51 (1973) 505; R. Carbonneau, P. Marmet, *Can. J. Phys.* 51 (1973) 2203; R. Carbonneau, P. Marmet, *Phys. Rev. A* 9 (1974) 1898.
- [19] P.J. Mohr, B.N. Taylor, *J. Phys. Chem. Ref. Data* 28 (1999) 1713; P.J. Mohr, B.N. Taylor, D.B. Newell, *Rev. Mod. Phys.* 80 (2008) 633.
- [20] R. Locht, B. Leyh, K. Hottmann, H. Baumgärtel, *Chem. Phys.* 220 (1997) 207; H. Keller-Rudek, G. K. Moortgat, MPI-Mainz-UV-VIS Spectral Atlas of Gaseous Molecules, <http://www.atmosphere.mpg.de/spectral-atlas-mainz>.
- [21] H. Jiang, D. Appadoo, E. Robertson, D. McNaughton, *J. Comput. Chem.* 23 (2002) 1220.
- [22] R. Locht, D. Dehareng, B. Leyh, unpublished results.

[23] M.J. Berry, J. Chem. Phys. 61 (1974) 3114.

[24] S. Arulmozhiraja, M. Ehara, H. Nakasuji, J. Chem. Phys. 129 (2008) 174506.

[25] M.B. Robin, Higher Excited States of Polyatomic Molecules, vol. I, Academic Press, New York, 1974.

[26] R.F. Lake, H. Thompson, Proc. Roy. Soc. Lond. A315 (1970) 323.

[27] E. Lindholm, Arkiv Fysik 40 (1969) 97.

[28] R. Locht, B. Leyh, A. Hoxha, H.W. Jochims, H. Baumgärtel, Chem. Phys. 272 (2001) 259; R. Locht, B. Leyh, H.W. Jochims, H. Baumgärtel, Chem. Phys. 317 (2005) 73; R. Locht, B. Leyh, H.W. Jochims, H. Baumgärtel, Chem. Phys. 365 (2009) 109.

[29] U. Fano, Phys. Rev. 124 (1961) 1866.